LAWRENCE
LIVERMORE
NATIONAL
LABORATORY

UCRL-CONF-201244

Coherence Measurements of a Transient 14.7 nm X-ray Laser

J. Dunn, R.F. Smith, S. Hubert, M. Fajardo, P. Zeitoun, J.R. Hunter, C. Remond, L. Vanbostal, S. Jacquemot, J. Nilsen, C.L.S. Lewis, R. Marmoret, V.N. Shlyaptsev, M.F. Ravet, and F. Delmotte

November 26, 2003

SPIE – International Society for Optical Engineering conference on Soft X-ray Lasers and Applications V , San Diego, CA, August 3 – 8, 2003

Vol. 5197

Coherence Measurements of a Transient 14.7 nm X-ray Laser

J. Dunn [1], R. F. Smith [1], S. Hubert [2], M. Fajardo [3], P. Zeitoun [3], J. R. Hunter [1], C. Remond [2], L. Vanbostal [3], S. Jacquemot [2], J. Nilsen [1], C.L.S. Lewis [4], R. Marmoret [2], V.N. Shlyaptsev [5], M.F. Ravet [6], and F. Delmotte [6]

[1] Lawrence Livermore National Laboratory, Livermore, CA 94551
[2] Commisariat á l'Èngergie Atomique, BP 2, 91680 Bruyeres-le-Chatel, France.
[3] Laboratoire d'Interaction du rayonnement X avec la Matiére (LIXAM), Université Paris-Sud, Bât 350, 91405 Orsay, France.
[4] School of Mathematics and Physics, The Queen's University of Belfast, Belfast BT7 1NN, UK.
[5] Department of Applied Science, University of California Davis-Livermore, Livermore, CA 94551
[6] Laboratoire Charles Fabry de l'Institut d'Optique, Université Paris-Sud, France

ABSTRACT

We present the longitudinal coherence measurement of the transient inversion collisional x-ray laser for the first time. The Ni-like Pd x-ray laser at 14.68 nm is generated by the LLNL COMET laser facility and is operating in the gain-saturated regime. Interference fringes are produced using a Michelson interferometer setup in which a thin multilayer-coated membrane is used as a beam splitter. The longitudinal coherence length for the picosecond duration $4d^1S_0 \rightarrow 4p^1P_1$ lasing transition is determined to be ~400 μm (1/e HW) by adjusting the length of one interferometer arm and measuring the resultant variation in fringe visibility. This is four times improved coherence than previous measurements on quasi-steady state schemes largely as a result of the narrower line profile in the lower temperature plasma. The inferred gain-narrowed linewidth of ~0.29 pm is also substantially narrower than previous measurements on quasi-steady state x-ray laser schemes. This study shows that the coherence of the x-ray laser beam can be improved by changing the laser pumping conditions. The x-ray laser is operating at 4 – 5 times the transform-limited pulse.

Keywords: x-ray laser, longitudinal coherence, Michelson soft x-ray interferometry, EUV optics

1. INTRODUCTION

Since the early development of laboratory x-ray lasers, source coherence has been a very important parameter to fully realize the potential of many applications. Specifically, x-ray laser interferometry [1] and holography [2] have been demonstrated using the Nova Ne-like Y ion 15.5 nm and the Ne-like Se ion 20.6 nm laser lines, respectively. With the recent progress in saturated output, tabletop x-ray lasers operating at similar wavelengths, e.g. Ni-like Pd ion at 14.7 nm [3], many of the same applications that depend on the source coherence properties can be demonstrated on these smaller, higher repetition rate facilities. The longitudinal coherence, L_c, or temporal coherence, $t_c = L_c/c$ where c is the speed of light, of the source is inversely related to the spectral bandwidth, $\Delta\lambda$, and is a measure of the temporal separation along a beam in which the different spectral components maintain a phase relationship. This can yield important spectral linewidth and shape information and provide valuable insight into the lasing medium gain dynamics. Therefore, accurate measurements of x-ray laser longitudinal coherence and methods of improving the coherence are important for these applications as well as future design of extreme-ultraviolet (EUV) interferometers and high quality EUV optics.

The x-ray laser source longitudinal coherence length can be determined accurately from interferometry. Interference fringes will be generated in an amplitude division interferometer if the following prerequisites are satisfied: (1) The phase fronts of the two arms are spatially overlapped and co-propagated; (2) The arm lengths are equalized to an accuracy better than the coherence length of the source. Previous measurements of L_c were made on the NOVA Ne-like Y x-ray laser at 15.5 nm [4]. This quasi-steady state (QSS) scheme was generated with a single 500 ps pulse with several kilojoules of energy. The longitudinal coherence of this x-ray laser was measured to be ~100 μm (1/e HW), using a Mach-Zehnder type

interferometer with an inferred linewidth of 1.3 pm (FWHM) [4]. In an earlier NOVA experiment [5], a 1.1 pm (FWHM) linewidth for the Ne-like Se 20.6 nm x-ray laser, pumped by a 600 ps pulse, was measured directly using a high resolution spectrometer. In these QSS schemes, the duration of the x-ray laser pulse is typically shorter (~200 ps) [6] than the optical drive pulse, where the gain conditions are ultimately extinguished through over-heating and over-ionization of the high temperature plasma medium.

The transient collisional excitation x-ray laser [7] is a higher efficiency scheme suitable for laser drivers of less than 10 J energy. The strong inversion is pumped by a combination of a long ~ns prepulse with a short ~ps heating pulse where the duration of the very high gain ~65 cm^{-1} [3] is determined by the picosecond timescale over which the collisional pumping takes place. The picosecond output makes this scheme well suited for probing fast evolving events [8]. In this paper, we describe transient x-ray laser measurements that have improved longitudinal coherence of ~400 μm (1/e HW) with an inferred gain-narrowed linewidth of ~0.29 pm (FWHM). The coherence length is approximately four times higher than the NOVA x-ray laser results mainly because of the lower plasma ion temperature in the optimized gain medium. The reported measurements in this work also show an improved coherence length and visibility when the short pumping pulse is lengthened from 6 ps to 13 ps.

2. EXPERIMENTAL DESCRIPTION

The Ni-like Pd 14.68 nm x-ray laser beam was generated using two laser beams at 1054 nm wavelength from the Compact Multipulse Terawatt (COMET) laser facility at LLNL [3]. Saturated x-ray lasing output in excess of 10 μJ was achieved with a combination of a 600 ps long pulse (2 J, 2×10^{11} W cm^{-2}) and a 13 ps (5 J, 3×10^{13} W cm^{-2}) main heating pulse. The short pulse arrived 700 ps peak-to-peak after the long pulse. For some shots the duration of the picosecond pulse was shortened to 6ps (5 J, 6×10^{13} W cm^{-2}). A 1.6 cm long line focus utilizing a 7-step traveling wave mirror geometry was used to irradiate a 1.25 cm long polished Pd slab target. This produced strong amplification in one axial direction where the output was collected by a multilayer optic. The experimental setup for generating the x-ray laser

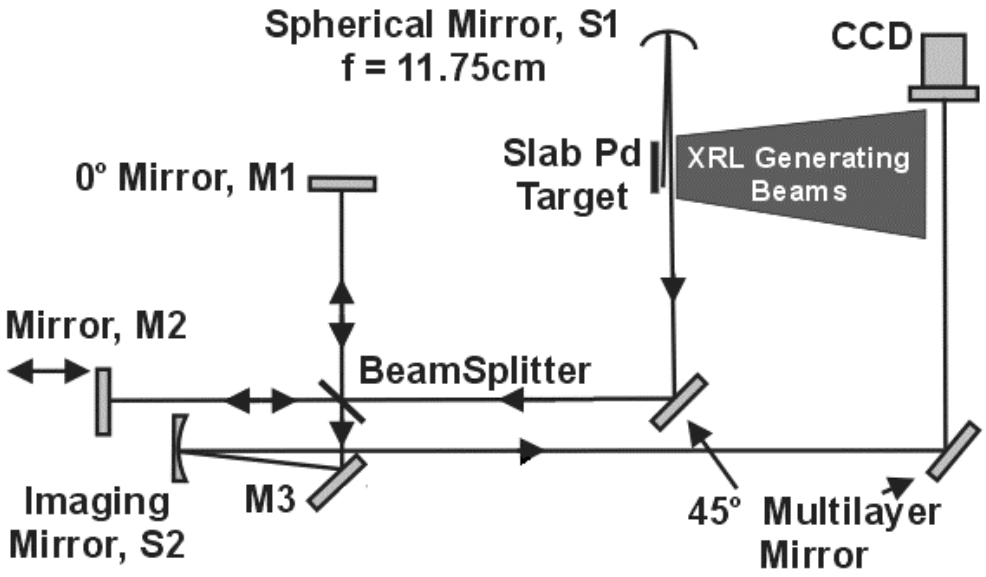

Figure 1: Experimental setup for 14.7 nm Michelson interferometer.

in relation to the Michelson interferometer is shown in Fig. 1. The x-ray laser output is imaged by a normal incidence Mo/Si multilayer spherical mirror (S1), with f = 11.75cm, and routed via a second flat 45° multilayer mirror, to the input path of the Michelson interferometer. The x-ray laser interacts with the first component, a thin foil beamsplitter (BS), which is partially transmissive and partially reflective at the 14.68 nm wavelength. The beamsplitter consists of an 89 nm thick Si_3N_4 membrane (active area of 0.5 × 0.5 cm^2) coated either side with 4.5 bi-layers of Mo/Si. The reflectivity and transmission at the x-ray laser wavelength is 0.144 and 0.151, respectively. The two arms, 34 cm in length and equal to better than 0.1 cm, of the interferometer are defined by the normal incidence 0° multilayer optics, M1

and M2, and the beam splitter. Interference fringes are generated by adjusting the spatial overlap and length of one arm with the M2 mirror which has motorized yaw, pitch and translation. The estimated throughput of the interferometer is approximately 0.007 per arm. The output beam from the interferometer reflects off M3 onto a spherical multilayer imaging mirror, S2 (f = 50cm), and is then relayed, via a 45° multilayer optic, to a back-thinned charged-coupled device (CCD) detector with a 1024×1024 (pixel size 24×24 μm^2) array. The S2 mirror is set to image a plane, within the M1 arm, where a laser-produced plasma can be generated for pump-probe experiments. The total magnification of the imaging system is estimated to be ~7.5 times giving a pixel limited resolution of 3.2 μm at the target plane. The x-ray laser output is effectively relay imaged, via S1 and S2, to the CCD detector plane with a total magnification of ~150 times.

3. EXPERIMENTAL RESULTS FROM THE MICHELSON INTERFEROMETER

Figure 2 shows a sample interferogram and lineout. The image captured by the CCD camera represents a region of ~1700 × 1700 μm^2 at the target plane (positioned inside the arm BS-M1) and encompasses the entire exit pattern of the x-ray laser beam. This image is taken with the interferometer alignment optimized and the path length of BS-M2 set to give the best fringe visibility (ΔL = 0). The curvature associated with the fringes is due to stresses across the beamsplitter causing local variations in the angles of the phase front within the x-ray beam. The variation in the fringe separation

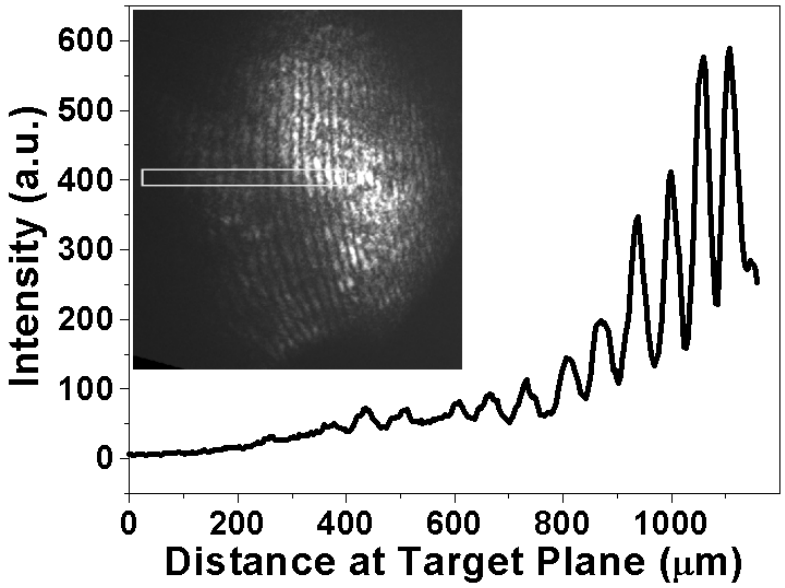

Figure 2: Interferogram with intensity lineout taken at optimum interferometer alignment, ΔL = 0. Short pulse is 13 ps pulse showing good fringe visibility over several hundred microns.

across the beam is also a function of this angular offset and has been discussed previously [4]. Fringe visibility, $V = (I_{max} - I_{min})/(I_{max} + I_{min})$, up to 70% is measured in some regions of the interferogram. Larger-scale intensity variations across the image are due to transverse spatial mode structure of the x-ray laser beam as confirmed in earlier near-field imaging experiments. There exists good coherent relationship between the modes after equalization of the interferometer arms. Some smaller scale structure along individual fringes is observed which may be due to non-uniformities within the beamsplitter or multilayer optics.

4. LONGITUDINAL COHERENCE MEASUREMENTS

The longitudinal coherence of the source is determined by adjusting the path difference (ΔL) between the two arms of the interferometer using the encoded translation stage of M2. The fringe visibility in the interferograms is then measured for both a 6 ps and a 13 ps short laser pulse to generate the x-ray laser. The other laser conditions remained constant. The results are shown in Fig. 3. It was found that for increasing values of ΔL, regions in which good fringe quality was observed became more localized indicating spatial variation of the longitudinal coherence across the x-ray laser beam.

Each data point in Fig. 3 signifies the average of the nine highest visibility measurements across a single interferogram. Fringe visibility below 0.2 was difficult to quantify at larger values of ΔL because the fringe continuity reduced to a scale less than the integration window. The overall value of 50% visibility is due to unequal throughput for the two arms. No

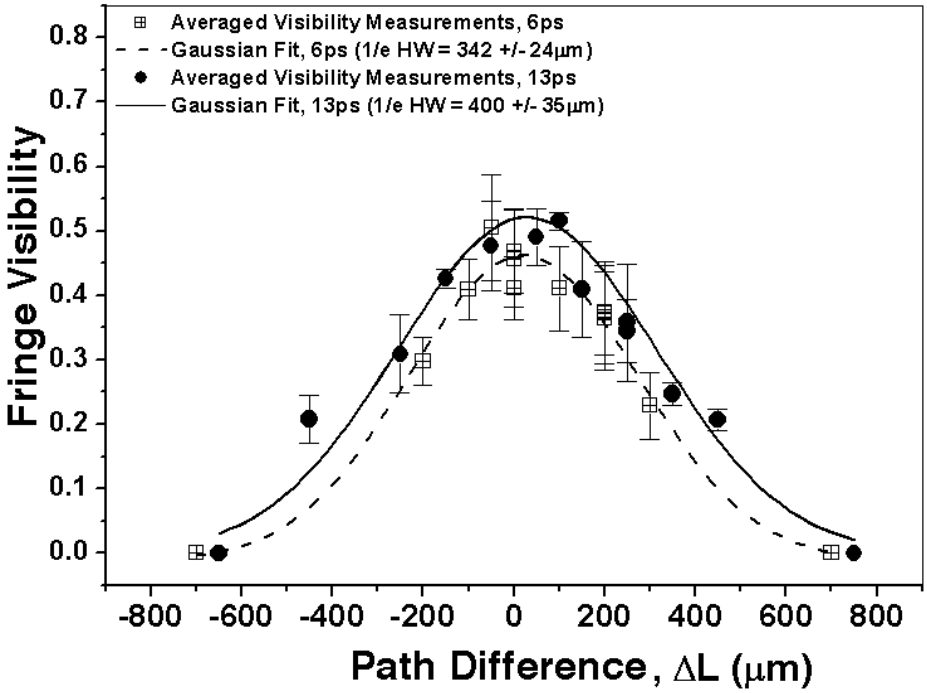

Figure 3: Variation of fringe visibility with path difference between two arms of the interferometer for 6 ps (open symbols) and 13 ps (closed symbols) heating pulse. Each data point is average visibility for a given shot taken from nine separate measurements across the interferogram. Error bars represent one standard deviation. The data points are fit by a Gaussian curve with a 1/e half width (HW) of 400 μm ± 35 μm (solid line, 13 ps) and 342 μm ± 24 μm (dashed line, 6 ps).

fringes were observed for ΔL above ±750 μm. A Gaussian fit gives very good agreement to the data with a 1/e half width (HW) of 400 μm ± 35 μm for the 13 ps pumping pulse and 342 μm ± 24 μm for the 6 ps pulse. It may be noted that the x-ray laser intensity, fringe uniformity and visibility were better with the longer pumping pulse. In each case the x-ray laser output was in the saturation regime.

Interpretation of the experimental data can be treated as follows. The measured fringe visibility is equal to the magnitude of the complex degree of coherence within the illumination beam [9]. This is a measure of the degree of correlation between the two combining phase fronts at the output of the interferometer. The complex degree of coherence is shown to be related to the power spectral density of the x-ray laser pulse, I(υ), utilizing the Fourier transform relationship of Wiener-Khintchine theorem [10]. As a result, the linewidth $\Delta\upsilon$ (FWHM) and the coherence time τ_c are inversely related. There is sufficient evidence from Fig. 3 to assume that the x-ray laser line has a Gaussian power spectrum where the intensity dependence on frequency follows $I(\upsilon) \propto \exp\{-[2\sqrt{\ln(2)}(\upsilon - \upsilon_0)/\Delta\upsilon]^2\}$, where $\Delta\upsilon$ is the line width of the lasing transition, $\upsilon_0 = c/\lambda$. The phase front associated with one arm is delayed by a time $\tau = 2L/c$ when the M2 arm is moved by a distance L. The measured fringe visibility dependence on τ, $V(\tau)$, is then the envelope of the autocorrelation function of the power spectrum varying as, $V(\tau) = \exp\{-[\pi\Delta\upsilon\tau/(2\sqrt{\ln(2)})]^2\}$. The coherence time, τ_c, is defined as the value of τ where the visibility has been reduced to 1/e the maximum value. From the Gaussian fits mentioned above, a spectral linewidth of ~0.34 pm and ~0.29 pm (FWHM) is determined for the 6 ps and 13 ps x-ray laser heating pulse, respectively. This corresponds to a spectral resolution $\lambda/\Delta\lambda \sim 4.3 \times 10^4$ and 5.06×10^4, respectively. These line widths are narrow and confirm the expected highly monochromatic nature of the x-ray laser. It is important to note that the longitudinal coherence measurements from the average visibility plot are the maximum value from the distribution within the x-ray laser total spatial beam profile.

In order to compare these line widths, simulations of the x-ray laser medium conditions were carried out with the 1-D LASNEX hydrodynamics and CRETIN atomic kinetics code [11] for the 13 ps heating pulse. From these calculations it is predicted that the ion temperature remains constant (± 10%) within the spatial region of the gain profile and for a time period longer than the gain duration, see Fig. 4. This is supported by the near field imaging results that indicate the x-ray laser is strongly amplified through the region 20 – 50 μm from the target surface. For the predicted ion temperature of 35 eV the Doppler broadened line shape can be calculated from $\lambda/\Delta\lambda = 1.2961 \times 10^4 [M/T_i]^{1/2}$, where M is the Pd ion

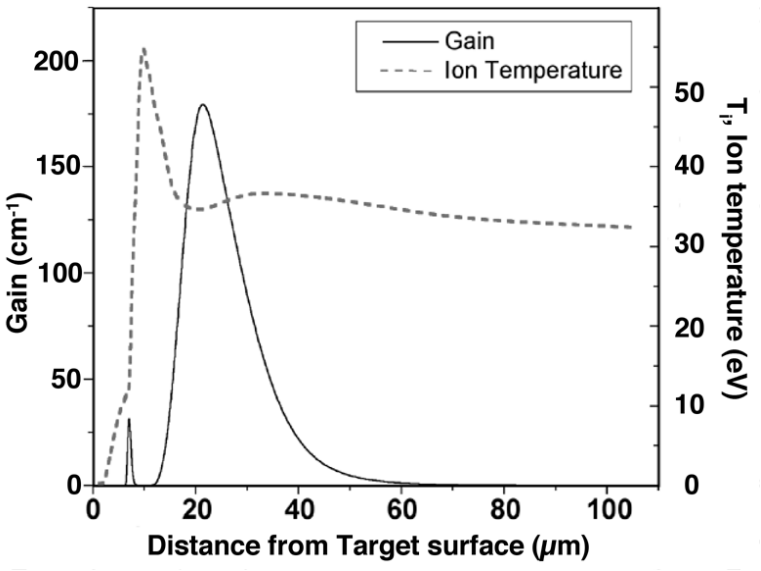

Figure 4: 1-D LASNEX and CRETIN simulations for the Ni-like Pd gain (solid line, left axis) and ion temperature, T_i, (dashed line, right axis) as a function of distance from the target surface. The laser conditions are 600 ps long pulse (1.5 J, 10^{11} W cm^{-2}) and a 13 ps (5 J, 2.3×10^{13} W cm^{-2}) where the 13 ps pulse arrives 700 ps after the peak of the long pulse. This is for conditions just after the peak of the short laser pulse.

mass (atomic mass units) and T_i is the ion temperature (eV). For Pd where M = 106.4 amu and T_i = 35 eV, the thermal Doppler line width is equivalent to ~0.65 pm (FWHM). This is approximately a factor of two larger than the results from the coherence measurements. It is expected that gain narrowing of the Doppler broadened line would occur and the gain-narrowed width would scale as $\sim(gl)^{-1/2}$, where g is the small signal gain and l is the length of the gain medium [5]. Previously measured gain-length products of 18 [3] would narrow the predicted Doppler broadened lineshape to ~0.15 pm. It can be noted that this is a low temperature plasma and other line mechanisms [5] would be expected to bring this figure into closer agreement with the experimental measurements. Additional RADEX simulations confirm that the plasma ion temperature during x-ray laser amplification is in the range of T_i = 35 – 40 eV, but also shows that the Doppler broadening mechanism contributes approximately 50 – 55% of the total line width which is ~1.3 pm *before* gain narrowing is considered. When gain narrowing is taken into account, the agreement is closer. This indicates that a full treatment of all line broadening mechanisms including Stark effects together with natural line shape as well as operation in the gain-narrowed bandwidth regime would be required.

5. TRANSFORM-LIMITED PULSE DISCUSSION

Recently it has been reported that picosecond driven x-ray lasers may be operating in a close to transform-limited or bandwidth-limited regime [12, 13] where the narrow spectral bandwidth of the x-ray laser places a fundamental limit on the shortest pulse duration. This phenomenon is well-documented in the area of ultrafast pulse generation within the laser community [14–16]. In fact, the shape and frequency bandwidth of the laser spectra in chirped pulse amplification systems is often controlled and increased to generate progressively shorter femtosecond pulses [17]. We have an estimate of the spectral line shape and width in this work together with an x-ray laser pulse duration measurement for similar

pumping pulse conditions [18]. This allows an accurate determination of the degree of transform limited operation for the Ni-like Pd ion x-ray laser line at 14.7 nm.

For the wave nature of light, time t and frequency υ are conjugate. This means that for a wave with a pure single frequency, the frequency bandwidth would be infinitely narrow but temporally would last for an infinite time. In reality, limiting the pulse duration will introduce a frequency spread in the wave, and *vice-versa*. Fourier analysis or Fourier transforms can be applied to the pulse shape to give the formula for the time-bandwidth product $\Delta\upsilon\ \Delta t \geq 1$. The value of the right-hand side of this expression depends on the exact pulse shape, definition of Δ and whether it refers to the full width at half maximum (FWHM), the full width at *1/e* intensity or the root mean square of the function [14]. Another consideration for the time-bandwidth product, is the level of chirp or other amplitude or phase substructure contained within the pulse [14]. Pulses without additional chirp or other substructure would be expected to be transform-limited. For this analysis, the common FWHM definition will be applied and for the sake of completeness various pulse shapes will be considered to illustrate the extent of the transform limit regime in each case.

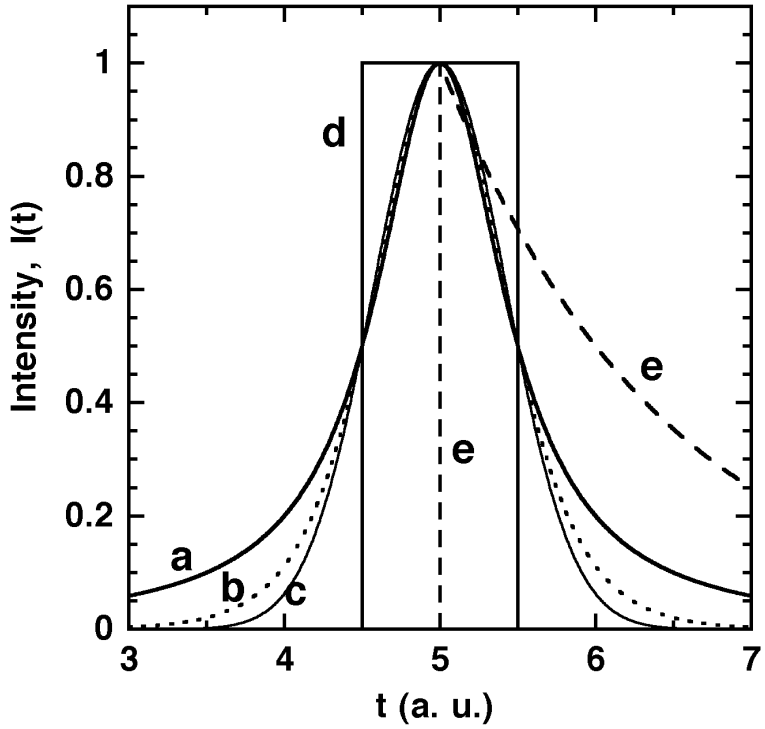

Figure 5: Plot of five different pulse shapes and intensity profile with peak intensity of unity and FWHM, $\Delta t = 1$. Peaks are centered at t =5. Curves are labeled as follows: (a) Lorentzian (solid line), (b) $Sech^2$ hyperbolic secant squared (dotted line), (c) Gaussian (solid line), (d) Flat top (solid line), and (e) single-sided exponential (dashed line).

Figure 5 shows a plot of the intensity profile *I(t)* for five different pulse shapes under consideration: Gaussian, Lorentzian, $sech^2$ (hyperbolic secant squared), flat-top and a single-sided exponential. They are normalized to have a peak intensity and a FWHM of unity. Table 1 below lists the functions, the corresponding intensity profile *I(t)*, and the time-bandwidth product $\Delta\upsilon\ \Delta t$ [14–16]. It can be seen that the transform-limit is different for each pulse shape. For this work, the spectral shape is Gaussian and similarly the measured temporal pulses are frequently Gaussian in profile [18]. From Table 1, the Gaussian profile has a time-bandwidth product $\Delta\upsilon\ \Delta t = 0.441$. For the 6 ps pumping pulse, the spectral

Table 1. Pulse shape, intensity profile parameters and transform-limited product

Pulse Shape	**Intensity Profile, I(t)**	**Time-Bandwidth** [a] $\Delta\upsilon\ \Delta t =$
(a) Lorentzian	$[1 + (2t/\Delta t)^2]^{-1}$	0.221
(b) $Sech^2$ [b]	$\cosh^{-2}(1.76t/\Delta t)$	0.315
(c) Gaussian	$\exp(-4\ (\ln 2)\ (t/\Delta t)^2)$	0.441
(d) Flat Top	$1\ (\ 0 \leq t \leq \Delta t)$	0.886
(e) Single-sided exponential	$\exp(-(\ln 2)\ t/\Delta t),\ (t \geq 0)$	0.11

[a] Δt, $\Delta\upsilon$ are FWHM

[b] $\mathrm{sech}(t) = 1/\cosh(t) = 2/(e^t + e^{-t})$

width 0.34 pm is equivalent to a frequency $\Delta\upsilon$ of 4.73 × 10^{11} Hz (FWHM) with a transform-limit of 0.93 ps. The average saturated output x-ray laser pulse are in the range of 4.5 – 4.9 ps (FWHM). This is approximately 5 times the transform limit. Repeating the same analysis for the 13 ps data, 0.29 pm corresponds to $\Delta\upsilon$ of 4.04 × 10^{11} Hz (FWHM) with a transform-limit of 1.09 ps. The measured x-ray laser pulse widths for the 13 ps data are slightly longer with 5.89 ps (FWHM) mean value though values as short as 4.6 ps are measured. This again gives a 4 – 5 times transform limited pulse. It is probably not a coincidence that the measured time-bandwidth product $\Delta\upsilon\ \Delta t$ remains essentially constant for the two short laser pumping pulses. The observed "few times the transform-limited pulse" may also suggest that there is additional amplitude or phase structure in the pulse shape. It would seem that for 100 fs x-ray laser operation, broadening of the spectral line shape is required.

In comparison, for the previous NOVA experiments [4–6], the spectral bandwidth $\Delta\upsilon$ of 1.6 × 10^{12} Hz (FWHM) would generate a transform-limited pulse of 270 fs. The actual pulse widths were 200 ps and so were 700 times transform-limited.

6. CONCLUSIONS

We have reported new results for the longitudinal coherence of a picosecond laser-driven transient x-ray laser [19]. The measured line width is a factor of four less than the 1.3 pm previously measured for the Ne-like Y quasi-steady state x-ray laser scheme [4]. In that work the predicted ion temperature of 600 eV was substantially higher than for the plasma conditions reported here, which directly affects the laser line width and coherence length. The improved coherence length in combination with the picosecond pulse duration makes this an excellent source for interferometry and holography applications. We also report that the x-ray laser is a few times the transform-limited pulse shape.

ACKNOWLEDGMENTS

The support and encouragement of Al Osterheld and Andy Hazi is greatly appreciated. These experiments were conducted at the Lawrence Livermore National Laboratory on the Physics and Advanced Technologies Directorate COMET laser facility. This work was performed under the auspices of the U.S. Dept. of Energy by the University of California Lawrence Livermore National Laboratory under Contract No. W-7405-Eng-48.

REFERENCES

1. L.B. Da Silva, T.W. Barbee, Jr., R. Cauble, P. Celliers, D. Ciarlo, S. Libby, R.A. London, D. Matthews, S. Mrowka, J.C. Moreno, D. Ress, J.E. Trebes, A.S. Wan, and F. Weber, "Electron Density Measurements of High Density Plasmas Using Soft X-Ray Laser Interferometry", *Phys. Rev. Lett.* **74**, 3991 (1995).
2. J.E. Trebes, S.B. Brown, E.M. Campbell, D.L. Matthews, D.G. Nilson, G.F. Stone, and D.A. Whelan, "Demonstration of X-ray Holography with an X-ray Laser", *Science* **238**, 517 (1987).
3. J. Dunn, Y. Li, A.L. Osterheld, J. Nilsen, J.R. Hunter, V.N. Shlyaptsev, "Gain Saturation Regime for Laser-Driven Tabletop, Transient Ni-Like Ion X-Ray Lasers", *Phys. Rev. Lett*. **84**, 4834 (2000).
4. P. Celliers, F. Weber, L.B. DaSilva, T.W. Barbee, Jr., R. Cauble, A.S. Wan, and J.C. Moreno, "Fringe formation and coherence of a soft-x-ray laser beam illuminating a Mach–Zehnder interferometer", *Opt. Lett.* **20**, 1907 (1995).
5. J. A. Koch, B. J. MacGowan, L. B. DaSilva, D. L. Matthews, J. H. Underwood, P. J. Batson, and S. Mrowka, "Observation of Gain-Narrowing and Saturation Behavior in Se X-Ray Laser Line Profiles", *Phys. Rev. Lett.* **68**, 3291 (1992).
6. L. B. Da Silva, B. J. MacGowan, S. Mrowka, J. A. Koch, R. A. London, D. L. Matthews, and J. H. Underwood, "Power measurements of a saturated yttrium x-ray laser", *Opt. Lett.* **18**, 1174 (1993).
7. P.V. Nickles, V.N. Shlyaptsev, M. Kalachnikov, M. Schnurer, I. Will, W. Sandner, "Short Pulse X-Ray Laser at 32.6 nm Based on Transient Gain in Ne-like Titanium", *Phys. Rev. Lett.* **78**, 2748 (1997).
8. R. F. Smith, J. Dunn, J. Nilsen, V. N. Shlyaptsev, S. Moon, J. Filevich, J. J. Rocca, M. C. Marconi, J. R. Hunter, and T. W. Barbee, Jr., "Picosecond X-Ray Laser Interferometry of Dense Plasmas", *Phys. Rev. Lett.* **89**, 065004-1 (2002).
9. P. W. Milonni and J. H. Eberly, *Lasers* (Wiley, New York, 1988), pp.559-562.
10. M. Born and E. Wolf, *Principles of Optics*, 7th ed. (Cambridge University Press, 1999), pp. 567.

11. J. Nilsen, J. Dunn, R.F. Smith, and T.W. Barbee, Jr., "Two-dimensional imaging and modeling of the 14.7 nm Ni-like Pd x-ray laser", *J. Opt. Soc. Am. B* **20**, 191 (2003).
12. Y. Abou-Ali, G.J. Tallents, M. Edwards, R.E. King, G.J. Pert, S.J. Pestehe, F. Strati, R. Keenan, C.L.S. Lewis, S. Topping, O. Guilbaud, A. Klisnick, D. Ros, R. Clarke, D. Neely, M. Notley, and A. Demir, "Measurement of the duration of X-ray lasing pumped by an optical laser pulse of picosecond duration", *Opt. Comm.* **215**, 397 (2003).
13. G.J. Tallents, Y. Abou-Ali, M. Edwards, Q. Dong, P. Mistry, G.J. Pert, C.L.S. Lewis, O. Guilbaud, A. Klisnick, D. Ros, D. Joyeux, and D. Phalippou, "Approaching the transform limit for x-ray laser pulses", these proceedings (2003).
14. A.E. Siegman, *Lasers* (University Science Books, Mill Valley, California, 1986) pp. 331 – 335.
15. E. P. Ippen, and C.V. Shank, *Ultrashort Light Pulses Picosecond Techniques and Applications* (Springer-Verlag, Berlin, 1977) ed. S.L. Shapiro, pp. 86 – 88.
16. W. Rudolph and B. Wilhelmi, *Light Pulse Compression* (Harwood Academic Publishers, Chur, Switzerland, 1989) pp. 1 – 8.
17. S. Backus, C.G. Durfee III, M.M. Murnane, and H.C. Kapteyn, "High power ultrafast lasers", *Rev. Sci. Instrum.* **69**, 1207 (1998).
18. J. Dunn, R.F. Smith, R. Shepherd, R. Booth, J. Nilsen, J.R. Hunter and V.N. Shlyaptsev, "Temporal characterization of a picosecond laser-pumped x-ray laser (for applications)", these proceedings (2003).
19. R.F. Smith, J. Dunn, J.R. Hunter, J. Nilsen, S. Hubert, S. Jacquemot, C. Remond, R. Marmoret, M. Fajardo, P. Zeitoun, L. Vanbostal, C.L.S. Lewis, M.-F. Ravet, F. Delmotte "Longitudinal Coherence Measurements of a Transient Collisional X-ray Laser", *Opt. Lett*. in press (2003).